Impact of Land-use Change on Surface Runoff in Manikin Basin et Kupang Regency

Arnoldus Nama, Yacob Victor Hayer and Fabianus Jawal S. Nope
Department of Civil Engineering, State Polytechnic of Kupang, Jl. Adisucipto, Penfui-Kupang, Indonesia

Keywords: Manikin Basin, Land Use Change, Image Classification, Soil and Water Assessment Tool, Runoff.

Abstract: The study assessed the impacts of land-use change on runoff in the Manikin Basin, using the Soil and Water Assessment Tool (SWAT) model. The model use to predict runoff for two scenarios. Both scenarios using different land-use data. Land-use for the SWAT model is obtained from remote sensing images. Two remote sensing images of Landsat 8 OLI from the years of 2014 and 2019 were used for land-use classification using the supervised classification method. The classification results show that there is a change in land-use. Area of land-use with the highest increase was shrubs with an increase of 20.25% (19.98 km^2), while the land-use area with the highest decrease was forest with a decrease of 14.1% (13.92 km^2). The average annual runoff of the first scenario is 134.7404, while the average annual runoff of the second scenario is 140.0596 mm, there is an increase of 3.98% (5.19 mm). This study shows that, the increase in the area of shrubs, and the reduction in forest area have an impact on increasing surface runoff in the Manikin watershed

1 INTRODUCTION

Watershed response to rainfall is determined by the characteristics of the watershed, including topography, soil moisture and type, land cover, and drainage density of the watershed. The topography and drainage density of the watershed are the physical characteristics of the watershed that do not change. In contrast to physical characteristics which tend to be static, biophysical characteristics such as land cover and soil interact dynamically. When these biophysical factors change, the surface runoff and flood discharge will also change as a watershed response to rainfall.

Research related to the impact of land-use changes on surface runoff has been conducted by several researchers. Patil, N. S. et. al. (2020), used the hydrological model (SWAT), to find out the effect of land-use change on surface runoff in the Hiranyakeshi watershed, India. Astuti I. S. et al. (2019), assessed the effect of land change on surface runoff using the SWAT model in the Upper Brantas watershed, Indonesia. Pertiwi, P. C. et. Al. (2020), analyzed the effect of land-use change on runoff discharge using the Nakayasu synthetic unit hydrograph (HSS) method in the Pompong watershed, Indonesia..

Research related to the impact of land-use change on surface runoff generally concludes that there is a relationship between both factors. However, it should be noted that the watershed response to rainfall differs from one watershed to another. Therefore, an analysis was carried out to understand the impact of land-use change on runoff in the Manikin watershed. The Soil and Water Assessment Tool (SWAT) hydrological model was used to predict surface runoff. The simulation of surface runoff in the Manikin watershed consists of two scenarios that are simulated with two different land-use data.

2 STUDY AREA

The study area (Fig. 1) is the Manikin River Basin in West Timor, East Nusa Tenggara Province, Indonesia. Manikin Basin has a catchment area of about 98.69 km2, with the longest channel reach from the upper basin of approximately 32 km to its outfall into Kupang bay.

According to the Schmidth-Fergudon climate classification, West Timor is dominated by climate type E, which is a slightly dry area with savanna forest vegetation. The rainy season in most of these areas is short of only 3-4 months, starting in December and ending in March or April. Annual rainfall varies from 848 mm on Panite, on the south

Nama, A., Hayer, Y. and Nope, F.
Impact of Land-use Change on Surface Runoff in Manikin Basin et Kupang Regency.
DOI: 10.5220/0010948700003260
In *Proceedings of the 4th International Conference on Applied Science and Technology on Engineering Science (iCAST-ES 2021)*, pages 526-533
ISBN: 978-989-758-615-6; ISSN: 2975-8246

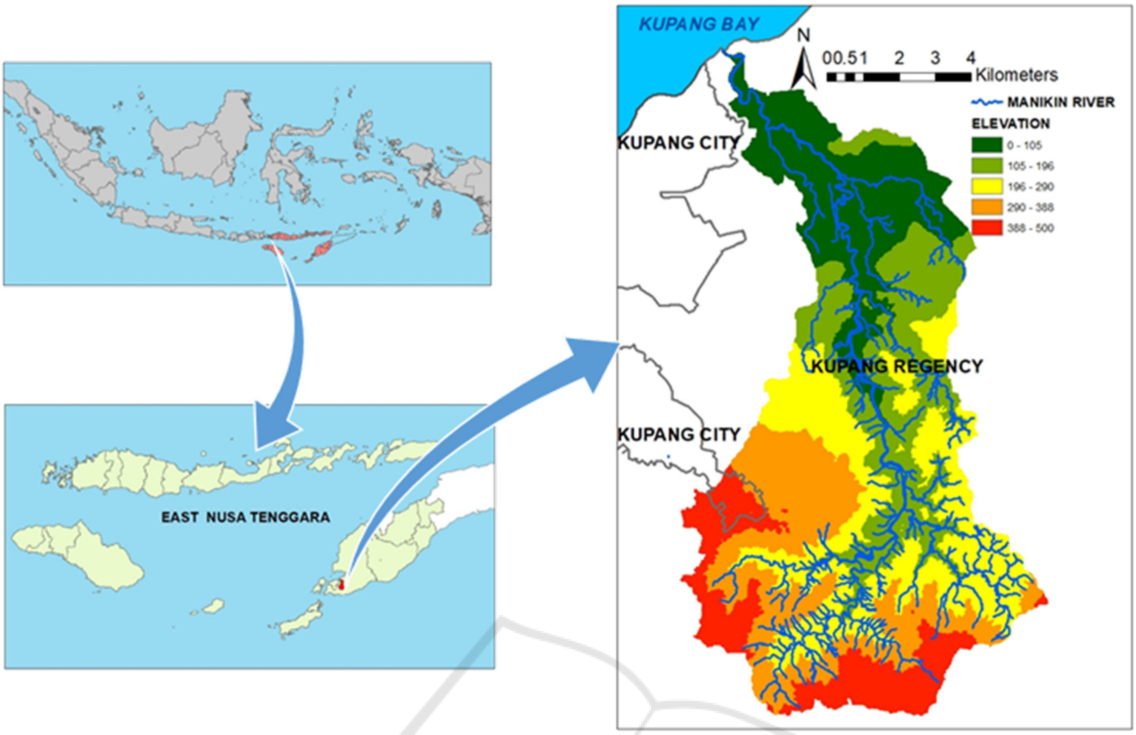

Figure 1: The Manikin Basin.

coast of Timor to 2,890 mm on Lahurus at the peak of Mount Lakaan, but most of West Timor receives 900-1,500 mm of rainfall per year, and Kupang (the provincial capital) and surrounding areas have an average rainfall of 900-1,500 mm. average rainfall is 1,420 mm per year.

The land cover in the manikin watershed is dominated by shrubs and savanna, while in the upper watershed there is little forest area. The settlement area is generally located in the downstream part of the watershed close to the Kupang City, slightly in the middle and upstream of the watershed.

3 MATERIALS AND METHODS

3.1 SWAT Model Description

The hydrological SWAT model used in this study is a predictive model for watershed-scale developed by Dr. Jeff Arnold for USDA Agricultural Research Service (ARS). SWAT was developed to predict the impact of land management practices on water, sediment, and agricultural chemicals that enter rivers or water bodies in a complex watershed with varying soil, land use, and management over a long period of time. SWAT models belong to a class of ecohydrological process-based watershed models, which can be defined as continuous dynamic models based on mathematical descriptions of physical, biogeochemical, and hydrochemical processes, incorporating elements of both physical and semi-empirical properties. The basic process model is not completely distributed in three dimensions, but usually includes a reasonable spatial disaggregation scheme, apply into sub-watersheds and hydrological response units (HRUs).

The basic SWAT model inputs are rainfall, maximum and minimum temperature, radiation, wind speed, relative humidity, land cover, soil, and elevation. The watershed is subdivided into sub-basins that are spatially related to one another, and, further, into hydrological response units (HRUs), which are homogenous units that possess unique land-use/land-cover and soil attributes and account for the complexity of the landscape within the sub-basins. The subbasin watershed components can be categorized as follows: hydrology, weather, erosion and sedimentation, soil temperature, plant growth, nutrients, pesticides, and land management. In the land phase of the hydrological cycle, runoff is predicted separately for each HRU. and routed to obtain the total runoff for the watershed.

In SWAT, surface runoff is most commonly predicted using the SCS curve number (SCS-CN) method, which was developed by the Soil

Conservation Service (now known as Natural Resource Conservation Service/NRCS). It calculates surface runoff according to the equation:

$$Q_{surf} = \frac{\left(R_{day} - I_a\right)^2}{\left(R_{day} - I_a + S\right)}$$

where Q_{surf} is the surface runoff (mm), R_{day} is the rainfall for the day (mm), I_a is the initial abstraction including surface storage, interception, and infiltration prior to runoff (mm), which is commonly approximated as $0.2S$, and S is a retention parameter.

The results of the SWAT model are calibrated with monthly discharge data of 2012 measurements, at locations near outlets. In the Manikin, river there is no discharge measurement station, and the existing discharge data is taken from manual measurements. Nash-Sutcliffe Efficiency (NSE) was used to test the reliability of the model. The NSE value of the test results is 0.776. Referring to Moriasi et. al, in Nama (2016), this model is very suitable to be applied in the Manikin Basin.

3.2 Data

The data used in this study include: (a) daily rainfall and temperature data – from Indonesian Meteorology and Geophysics Agency; (b) streamflow data – from Directorate General for Water Resources, Indonesian Ministry of Public Works (c) land cover – generated from Landsat 8 OLI satellite imagery (2014 and 2019); (d) soil map– from Indonesian Ministry of Agriculture; and (e) digital contour map in Esri format file (scale 1: 12500) from Indonesian geospatial information agency, used to generate digital elevation model (DEM).

3.3 Land-cover Assessment

Satellite imagery from Landsat 8 OLI (Operational Land Imager), were obtained from U.S. Geological Survey (USGS, http://earthexplorer.usgs.gov). There are two images, the first is a 2014 image, the date of recording (Date Acquired) 25 April 2014, and the second is the 2019 image, the recording date is 23 April 2019, with a path-row of 111-067 (Fig.2). This image covers the entire area of Kupang Regency, Rote Ndao Regency, and part of South Central Timor Regency, East Nusa Tenggara Province. This data is a free download from the USGS website (http://eartheexplorer.usgs.gov).

To obtain land use as input into the model, the software ENvironment for Visualizing Images (ENVI 5.1) and ArcGIS 10.5, was used to perform image analysis and classification. The ENVI software is used for image pre-processing, such as radiometric correction, noise reduction, and image sharpening. Image sharpening using the Gram-Schmidt Pan Sharpening method. To classify satellite images into land use maps, ArcGIS 10.5 software is used. Classification using the supervised technique with the maximum likelihood classification method. Seven land use classes were considered, namely: Grassland, Shrub, Water Body, Cornfield, Forest-Mixed, Paddy fields, and Residential-Medium Density.

Figure 2: The Landsat 8 OLI (*Operational Land Imager*) image *path-row* 111-067, True color.

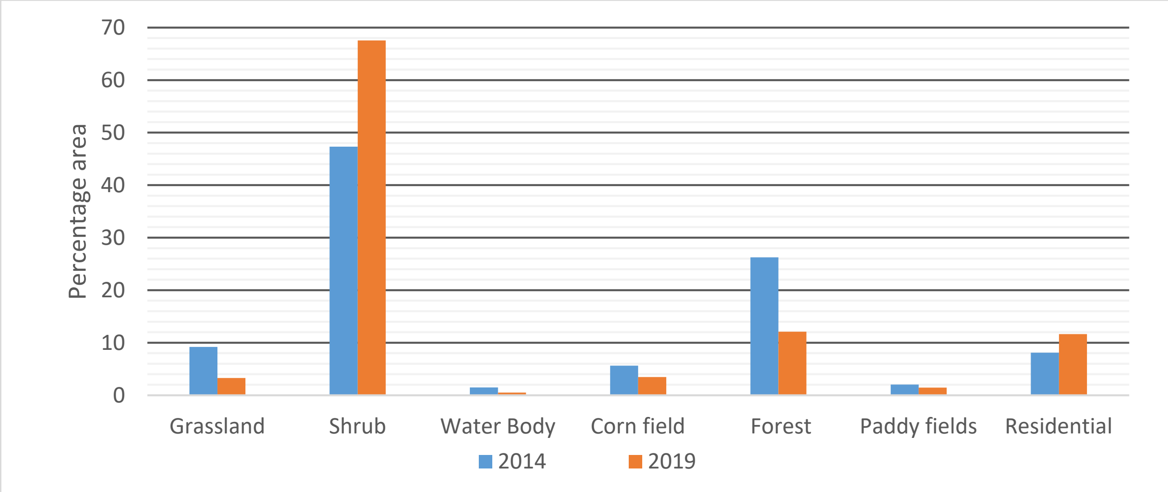

Figure 3: The comparison of land classes in 2014 and 2019.

Table 1: Land use in study area.

Land-use	2014		2019	
	Land area (Km^2)	% area	Land area (Km^2)	% area
Grassland	9.16	9.28	3.24	3.29
Shrub	46.68	47.3	66.67	67.55
Water Body	1.46	1.48	0.48	0.49
Corn field	5.56	5.63	3.42	3.47
Forest-Mixed	25.86	26.2	11.94	12.1
Paddy fields	1.99	2.02	1.44	1.46
Residential	7.98	8.09	11.49	11.64
Total area	98.69	100	98.69	100

4 RESULTS AND DISCUSSION

4.1 Image Analysis

Landsat Images were classified to land-use map using the Maximum Likelihood supervised classification method. Classification results are compared with observations. Verification was carried out at 34 locations in and around the watershed. Comparison of classification results and field conditions is used to calculate the level of accuracy in supervised interpretation, which is 85.29%.

The results of the classified images for the years 2014 and 2019 are shown in Table 1. The distribution of land classes in the watershed, for 2014 and 2019 respectively, is shown in Figure 3. As shown in Table 1, the residential land class experienced a significant increase from 8.09% to 11.64%. Meanwhile, the land classes that decreased in the area were grasslands and forests with changes of 9.2% to 3.29% and 26.2% to 12.1% respectively.

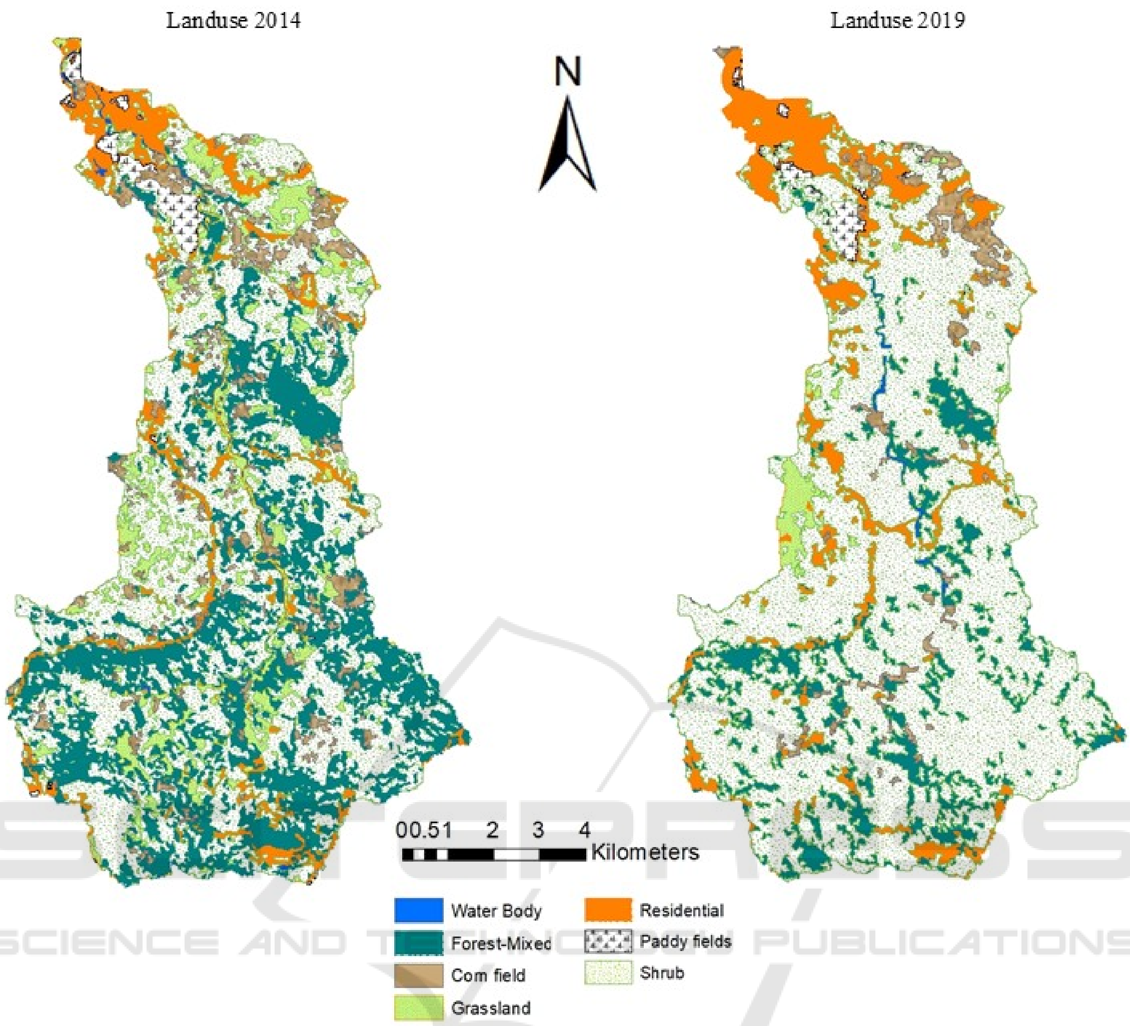

Figure 4: Land use class distribution on watershed for the year of 2014 and 2019.

4.2 Preparing Precipitation Data

Before the precipitation data is used, the consistency test is carried out using the multiple mass curve method. There are 4 precipitation stations in and around the watershed used for SWAT model input, namely Oeletsala, Baun, Tarus, and Penfui precipitation stations. The results of the consistency test of the four stations did not show any data inconsistency with the respective correlation coefficients above 0,99.

The next step is to do statistical calculations to arrange rain data in a format that can be read by the SWAT model. The statistical calculation of rain data includes (1) average amount of precipitation falling in month (PCPMM). (2) standard deviation for daily precipitation in month (PCPSTD), (3) skew coefficient for daily precipitation in month (PCPSKW), (4) probability of a wet day following a dry day in month (PR_W1), (5) probability of a wet day following a wet day in month (PR_W2), (6) average number of days of precipitation in month (PCPD), and (7) extreme half-hour rainfall for month (RAINHHMX).

WGN Parameters Estimation Tool software (downloaded for free at https://swat.tamu.edu) can be used to calculating Statistics of precipitation for swat model input. Overall results of the calculation of precipitation statistics are arranged according to a format that can be read by the SWAT model (SWAT version 2012), then inputted into the SWAT database (WGEN_user). An example of calculating rain statistics can be seen in Table 1.

Table 2: Statistical precipitation parameter of Tarus Rain gauge.

	Jan	Feb	Mar	Apr	May	Jun	Jul	Aug	Sep	Oct	Nov	Dec
PCPMM	309.0	444.9	267.9	87.6	18.0	5.9	4.8	1.4	1.9	17.8	138.8	245.2
PCPSTD	14.5	21.6	15.4	9.1	3.0	1.5	1.2	0.7	1.0	2.6	12.2	14.9
PCPSKW	1.9	1.7	2.6	4.9	6.9	12.5	11.1	16.1	16.3	5.5	3.6	3.5
PR_W1	0.5	0.5	0.3	0.2	0.0	0.0	0.0	0.0	0.0	0.1	0.2	0.4
PR_W2	0.7	0.9	0.8	0.5	0.4	0.5	0.5	0.3	0.3	0.2	0.5	0.7
PCPD	20.2	21.9	19.4	8.4	2.4	1.4	1.2	0.2	0.2	2.7	10.2	19.5
RAINHHMX	73.0	95.5	83.0	83.0	28.0	25.0	18.0	11.0	18.0	20.0	87.0	109.0

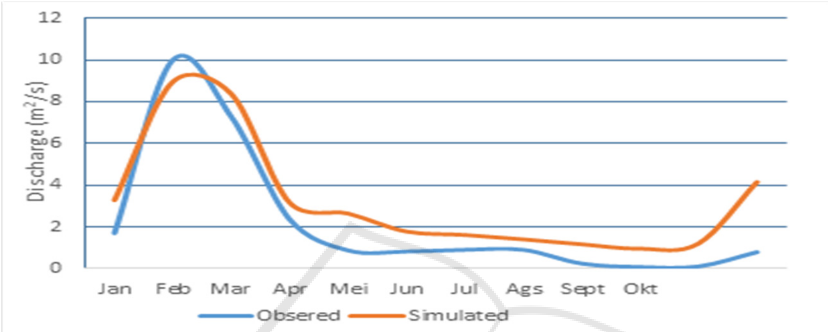

Figure 5: Graph of the relationship between the measurement discharge and the calibrated model discharge.

Table 3: The model evaluation statistics and performance.

Observed mean	St. dev	Simulated mean	St. dev	Cp	MAE	NSE	R^2
2.175	3.141	3.227	2.729	0.256	1.052	0.776	0.951

Table 4: Monthly run off.

	Jan	Feb	Mar	Apr	May	Jun	Jul	Aug	Sep	Oct	Nov	Dec
2014	18622	42078	39337	8274	4455	0.001	0.0	0.0	0.0	49	2093	18070
2019	19318	43593	40950	8583	4678	0.001	0.0	0.0	0.0	51	2171	18883

4.3 Hydrological Modelling

The output of a model after being calibrated must be evaluated statistically for the field data, although the graph of the output of the model after calibration and field measurements shows that the difference is not too significant. This is done to determine the suitability of the model with field data and to avoid too large a deviation between the model results and the field data. To test the reliability of the model, in this study several statistical indicators were used, namely the Correlation Coefficient (R2), Mean Absolute Error (MEA), Coefficient Performance (Cp), and Nash-Sutcliffe Efficiency (NSE). Figure 3 shows a graph of the relationship between the measurement discharge and the calibrated model discharge, while the results of the model reliability test presented in Table 2.

4.4 Runoff Depths

The output of the SWAT model simulation is discharge, runoff, total sediment, etc., however, the only runoff will be discussed here. The impact of land change on runoff can be seen in table 4 and table 5.

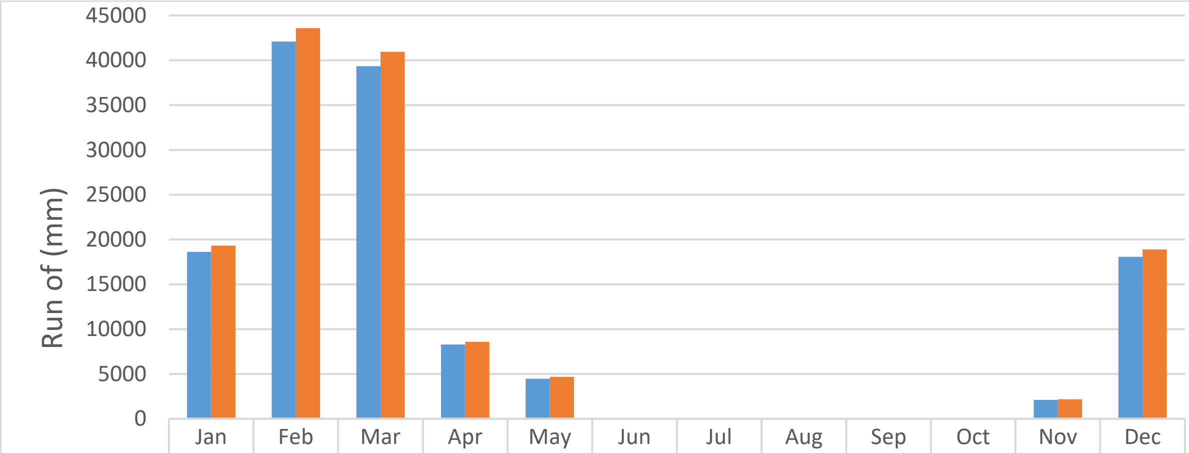

	Jan	Feb	Mar	Apr	May	Jun	Jul	Aug	Sep	Oct	Nov	Dec
Skenario 1	18621,5	42077,7	39336,8	8273,59	4455,28	0,001	0,000	0,000	0,000	49,204	2093,03	18069,6
Skenario 2	19317,9	43592,5	40949,6	8583,02	4678,05	0,001	0,000	0,000	0,000	51,123	2171,31	18882,8

Figure 6: Total monthly run of.

Table 5: Annual run off.

	Total (mm)	Average (mm)
2014	132977	134.7404
2019	138227	140.0596

As presented in Tables 4 and 5, there was an increase in runoff from the first scenario to the second scenario, both monthly and annual runoff. The largest total runoff for the two scenarios occurred in February, which was 43,593 mm, the lowest occurred in June, which was 0.001 mm. From July to September are period that are no rainfall in this area (dry season), therefore there is no runoff in this period. The average annual runoff for the first scenario is 134,7404 mm or about 8,279% of the total annual rainfall (mean annual rainfall is 1627,511 mm). For the second scenario, the average surface runoff is 140.0596 mm, or about 8.606% of the total annual average rainfall. From this description, the average runoff for the two scenarios is very small compared to the total average rainfall. This condition occurs because only storm rainfall cause runoff. The deep of rain that causes runoff requires further analysis.

There is an increase in annual runoff depth from the first scenario to the second scenario. Average annual runoff increased by 3.948% (5.19 mm). Area of land-use with the highest increase was shrubs with an increase of 20.25% (19.98 km^2), while the land-use area with the highest decrease was forest with a decrease of 14.1% (13.92 km^2). Shrubs and forest land-use classes have different runoff coefficients. The forest land-use class has a runoff coefficient that is lower than the shrubs land-use class. Increasing the area of shrubs and reducing the area of forest can increase runoff. Another factor that causes the increase in runoff is the increase in the area of residential areas.

5 CONCLUSION

This study shows that in five years, there has been a change in land use in the manikin basin. There are five land-use classes that decried in size, they were grasslands, water bodies, rice fields, and forests .The land classes that increased were residential land classes and shrubs. The average annual runoff of the first scenario is 134.7404, while the average annual runoff of the second scenario is 140.0596 mm. There is an increase in runoff depth from the first scenario to the second scenario, which is 3.98% (5.19 mm).

The Area of land-use with the highest increase was shrubs with an increase of 20.25% (19.98 km^2), while the land-use area with the highest decrease was forest with a decrease of 14.1% (13.92 km^2). The forest land-use class has a runoff coefficient that is lower than the shrubs land-use class, So, increase in the area of shrubs, and the reduction in forest area have an impact on increasing surface runoff in the Manikin watershed. Another factor that causes the increase in runoff is the increase in the area of residential areas. In general, this study shows that land-use change in the manikin basin from the year of 2014 to 2015 has effect on increase in the total runoff in the Manikin basin.

ACKNOWLEDGEMENTS

The leading author of this paper would like to thank to State Polytechnic of Kupang as a sponsor of the author's research through the State Polytechnic of Kupang DIPA fund.

REFERENCES

Asdak, C. (2004). *Hidrologi dan pengelolaan daerah aliran sungai*. Yogyakarta: Gajah Mada University Press.

Astuti I. S. et al. (2019). Impact of land use land cover (LULC) change on surface runoff in an increasingly urbanized tropical watershed. *Journal of Water Resources Management*, 33, 4087–4103

Krysanova, V. & White, M. (2015) Advances in water resources assessment with SWAT—an overview. *Hydrological Sciences Journal– Journal des Sciences Hydrologiques*, 60 (5).

Levin, N. (1999). *Fundamentals of Remote Sensing*. Trieste, Italy: Hydrographic Data Management course, IMO - International Maritime Academy.

Nama, A. (2016). Analisis Tingkat bahaya erosi dan arahan konservasi lahan dengan aplikasi GIS di DAS Manikin. *Jurnal Teknik Pengairan*, 7, 205-215

Neitsch, S. L., Arnold, J. G., Kiniry, J. R., Srinivasan, R., Williams, J. R. (2011). Soil and water assessment tool: Theoretical documentation version 2009. Texas, USA: Texas A & M University System College Station,

Nuri, R. (1985). *Geografi Budaya dalam Wilayah Pembangunan Nusa Tenggara Timur*. Jakarta: Departemen Pendidikan dan Kebudayaan Direktorat Sejarah dan Nilai Tradisional Proyek Inventarisasi dan Dokumentasi Kebudayaan Daerah

Patil, N. S. et. al. (2020). Effect of land use land cover changes on runoff using hydrological model: a case study in Hiranyakeshi watershed. *Modeling Earth Systems and Environment*, 6, 2345–2357

Pertiwi, P. C. et. Al. (2020). The effect of land use change to surface runoff discharge in the Pompong watershed at Bangka regency. 2nd International Conference on Green Energy and Environment (ICoGEE 2020)

Purwadhi, S. H., & Sanjoto, T. B. (2008). *Pengantar interpretasi citra penginderaan jauh*. Semarang: LAPAN & Universitas Negeri Semarang.